

## Dynamics of North Atlantic Deep Water masses during the Holocene

Babette A. A. Hoogakker,<sup>1,2</sup> Mark R. Chapman,<sup>3</sup> I. Nick McCave,<sup>1</sup> Claude Hillaire-Marcel,<sup>4</sup> Christopher R. W. Ellison,<sup>3</sup> Ian R. Hall,<sup>5</sup> and Richard J. Telford<sup>6</sup>

Received 12 April 2011; revised 14 July 2011; accepted 6 September 2011; published 19 November 2011.

[1] High resolution flow speed reconstructions of two core sites located on Gardar Drift in the northeast Atlantic Basin and Orphan Knoll in the northwest Atlantic Basin reveal a long-term decrease in flow speed of Northeast Atlantic Deep Water (NEADW) after 6,500 years. Benthic foraminiferal oxygen isotopes of sites currently bathed in NEADW show a 0.2‰ depletion after 6,500 years, shortly after the start of the development of a carbon isotope gradient between NEADW and Norwegian Sea Deep Water. We consider these changes in near-bottom flow vigor and benthic foraminiferal isotope records to mark a significant reorganization of the Holocene deep ocean circulation, and attribute the changes to a weakening of NEADW flow during the mid to late Holocene that allowed the shoaling of Lower Deep Water and deeper eastward advection of Labrador Sea Water into the northeast Atlantic Basin.

**Citation:** Hoogakker, B. A. A., M. R. Chapman, I. N. McCave, C. Hillaire-Marcel, C. R. W. Ellison, I. R. Hall, and R. J. Telford (2011), Dynamics of North Atlantic Deep Water masses during the Holocene, *Paleoceanography*, 26, PA4214, doi:10.1029/2011PA002155.

### 1. Introduction

[2] The formation of deep waters in the Labrador and Nordic Seas, a key component of the Atlantic Meridional Overturning Circulation (AMOC), plays an important part in the oceanic distribution of salt and heat. In addition, the process of cooling and convection of surface waters at high latitudes isolates CO<sub>2</sub> from the atmosphere. Although the major features and global significance of AMOC are now fairly clear, the magnitude and time scales of natural variability in ocean circulation remain uncertain, making inferences of future ocean heat transport and absorption of CO<sub>2</sub> insecurely based. One route toward improvement of these predictions is via documentation of the magnitude of recent changes in ocean circulation during the present relatively ice-free interglacial. Several studies have shown that AMOC strength may have been reduced during the Holocene for short intervals that lasted between 100 and 1000 years [Bianchi and McCave, 1999; Oppo *et al.*, 2003; Hall *et al.*, 2004; Ellison *et al.*, 2006; Kleiven *et al.*, 2008]. On a longer time-scale, a weakened AMOC has been proposed as a potential explanation for deep ocean carbonate ion

concentrations that are lower than expected accompanying a 20 ppmv rise in atmospheric CO<sub>2</sub> from ca. 8,000 years [Broecker and Clarke, 2007], but so far there is no independent proof for such a weakening. Here we show evidence for a long-term weakening of the input flow of one of the two principal components of North Atlantic Deep Water during the Holocene and link this to shoaling of Lower Deep Water (LDW), sourced from Antarctic Bottom Water (AABW), and deeper eastward advection of Labrador Sea Water (LSW) into the northeast Atlantic Basin.

### 2. Cores, Methods, and Age Models

[3] We have reconstructed deep water properties and circulation strength for the last 10,000 years, using silt particle size [McCave and Hall, 2006] and benthic foraminiferal oxygen isotopes ( $\delta^{18}\text{O}_c$ ). High resolution records of flow speed vigor were generated for two locations (Figure 1): (1) piston core MD95–2024 and box core HU91–045–093 at Orphan Knoll in the southern Labrador Sea (50.208°N, 45.688°W) at 3448 m water depth (hereafter collectively referred to as MD2024) and (2) piston core MD99–2251 from the Gardar Drift (57.458°N, 27.913°W) at 2620 m water depth (hereafter referred to as MD2251), using the mean grain size of the sortable silt fraction ( $\overline{SS}$ ; 10–63  $\mu\text{m}$  terrigenous fraction) as a physical proxy for near-bottom flow speed [McCave *et al.*, 1995].

[4] All samples were analyzed for particle size using a Coulter Multisizer II. Prior to analysis samples were treated with dilute acetic acid (1 M) and heated sodium carbonate (2 M) to remove calcium carbonate and biogenic opal. The Coulter counter gives a more precise measure although smaller dynamical range compared to a Sedigraph [Bianchi

<sup>1</sup>Department of Earth Sciences, University of Cambridge, Cambridge, UK.

<sup>2</sup>Now at School of Geographic Sciences, University of Bristol, Bristol, UK.

<sup>3</sup>School of Environmental Sciences, University of East Anglia, Norwich, UK.

<sup>4</sup>Centre GEOTOP, Université du Québec à Montréal, Montreal, Canada.

<sup>5</sup>School of Earth and Ocean Sciences, University of Cardiff, Cardiff, UK.

<sup>6</sup>Department of Biology, University of Bergen, Bergen, Norway.

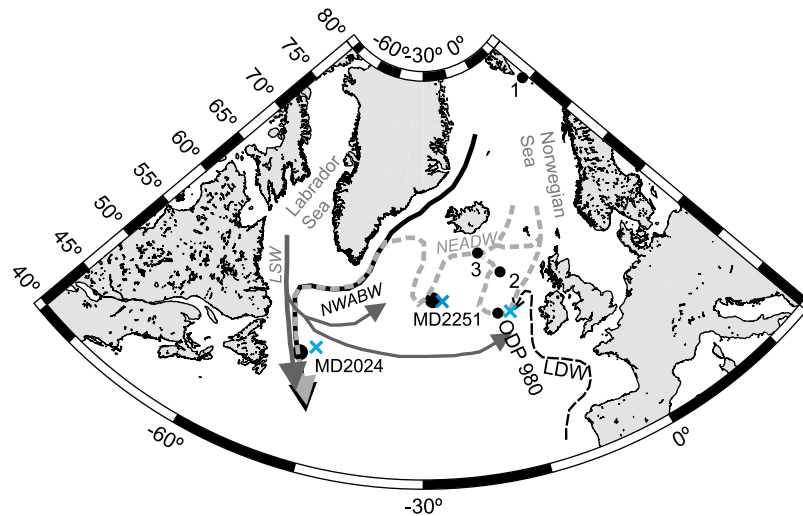


**Figure 1.** Map showing deep water flow paths in the North Atlantic and location of the cores used in this study. In addition to the flow paths of NEADW, NWABW and LSW we also indicate the flow path of Lower Deep Water (LDW). Core MD2024 is located at Orphan Knoll in the Labrador Sea; core MD2251 in the northeast Atlantic, near the Reykjanes Ridge on Gardar Drift; core ODP 980 [Oppo *et al.*, 2003] in the northeast Atlantic, SE of Rockall Plateau on Feni Drift. Numbers 1 to 3 indicate locations of cores 23258–3 [Sarnthein *et al.*, 2003], BOFS17K [McCave, 1989; Bertram *et al.*, 1995], and RAPiD-12-1K [McCave, 2005; Thornalley *et al.*, 2010] respectively. Location details can be found in Table 1. Blue crosses (online version) indicate locations of hydrographic stations used to create temperature and salinity profiles in Figure 2.

*et al.*, 1999; McCave and Hall, 2006]. The sortable silt concentrations exceeding 5% found here give precisions of  $\pm 1.5\%$  [Bianchi *et al.*, 1999].

[5] Benthic  $\delta^{18}\text{O}_c$  records are based on analysis of epi-faunal *Cibicidoides wuellerstorfi*. The benthic foraminiferal isotope record of ODP Site 980 on Feni Drift (55.483°N; 14.702°W) [Oppo *et al.*, 2003] at 2.2 km water depth to the east of core MD2251 (Figure 1), was used to monitor deep water characteristics, as specimens are too sparse in MD2251. For MD2024  $\delta^{18}\text{O}_c$  ratios were measured on an average of 5 specimens in the 150–300  $\mu\text{m}$  fraction, using a VG Prism mass spectrometer with a “multiprep” system. Prior to analysis, specimens were cleaned using hydrogen peroxide. Calibration to VPDB was via the NBS19 standard. The analytical precision was  $\pm 0.08\%$  for  $\delta^{18}\text{O}_c$ . A total of 242 analyses were carried out, including 25 duplicate measurements. The duplicate  $\delta^{18}\text{O}_c$  measurements on samples differed by an average of 0.06‰ (combining both analytical and within-sample variability). We compare the benthic  $\delta^{18}\text{O}_c$  record of Feni Drift with benthic foraminiferal  $\delta^{13}\text{C}$  of Feni Drift and the Norwegian Sea in order to make inferences of potential source water changes.

[6] We have not included benthic foraminiferal  $\delta^{13}\text{C}$  data for the Labrador Sea site MD2024 because local productivity factors appear to exert a major control. Benthic foraminiferal  $\delta^{13}\text{C}$  records from the Labrador Sea show depleted values (0.5‰ [Kleiven *et al.*, 2008]) between 10,000 and 7,500 years compared with northeast Atlantic records (auxiliary material).<sup>1</sup> At the same time productivity (especially that of diatoms) in the Labrador Sea was very high [Radi and de Vernal, 2008].

<sup>1</sup>Auxiliary materials are available in the HTML. doi:10.1029/2011PA002155.

As there was no increase in organic carbon burial [Hillaire-Marcel *et al.*, 1994], it is likely that the early Holocene depleted benthic foraminiferal  $\delta^{13}\text{C}$  values from the Labrador Sea are the result of remineralization resulting from this increased organic material flux, rather than a shoaling of LDW in the West Atlantic Basin. The absence of a similar foraminiferal  $\delta^{13}\text{C}$  signal in a deeper site (CH 69-K09 by Laybeyrie *et al.* [2005]) in the NW Atlantic Basin, which presently contains a much larger contribution of LDW also is not consistent with shoaling of LDW. Core MD2024 has relatively enriched benthic foraminiferal oxygen isotopes ( $\sim 3\%$ ) throughout the Holocene which are indicative of a high Northern Latitude source rather than a Southern Ocean source [Schmidt *et al.*, 1999]. Finally, neodymium isotope data from Blake Outer Ridge at 4250 m in the West Atlantic Basin shows the least radiogenic values during the early Holocene, confirming a distinct dominance of NADW there [Gutjahr *et al.*, 2008]. Epi-benthic foraminiferal  $\delta^{13}\text{C}$  from the Labrador Sea are therefore not included in our discussion.

[7] The age models of cores MD2024 and MD2251 are both based on generalized mixed effect regressions, using mid-point estimates of calibrated radiocarbon ages, following Heegaard *et al.* [2005]. For box-core HU-091-045-09 linear interpolations between the core top (assigned 0 years BP) and two calibrated radiocarbon ages were applied. A simple linear projection between the two radiocarbon ages at 29 cm (1,860 years) and 43 cm (2,520 years) gives an age of  $\sim 500$  years for the core top. However, bearing in mind the dating uncertainties, it’s only a two-point projection, and with no evidence for erosion in the box core, we regard the assumption of a core top age of zero as reasonable. Radiocarbon ages for both sites were obtained from monospecific samples of the planktonic foraminifer *Globigerina bulloides*.

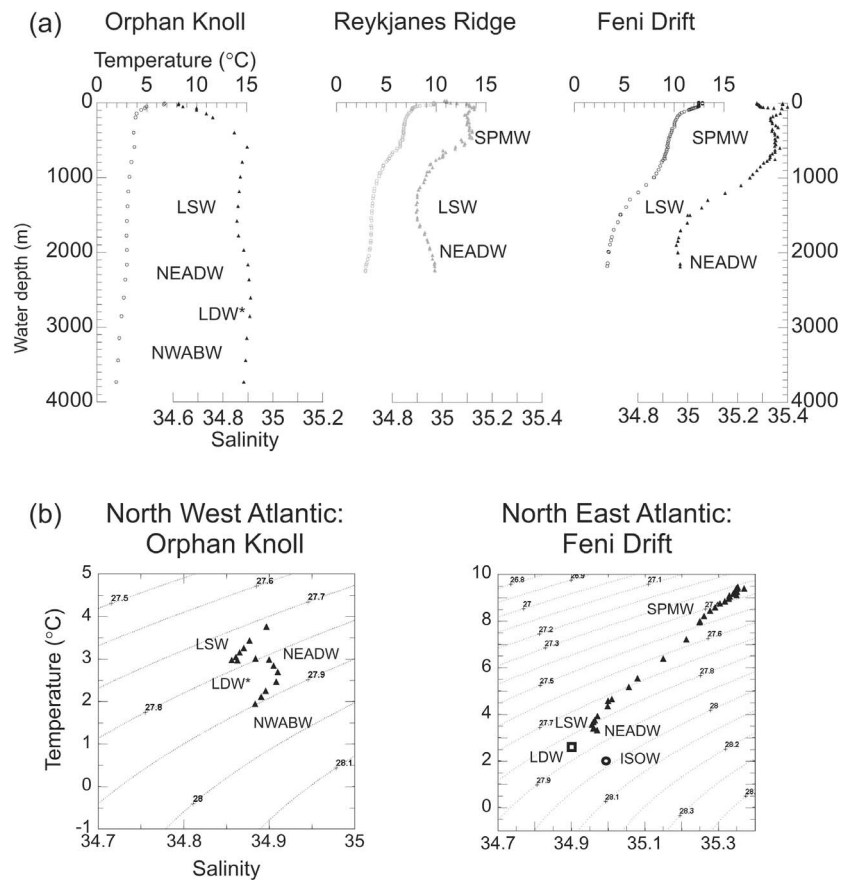


**Figure 2.** (a) Seawater temperature (circles) and salinity (triangles) profiles near Orphan Knoll (in the Labrador Sea), Gardar Drift (Reykjanes Ridge) and Feni Drift (Rockall Plateau) [Boyer *et al.*, 2006], showing characteristics of the main deep and intermediate North Atlantic water masses. Location details of the hydrographic stations can be found in Figure 1. In the Labrador Sea a layer containing enhanced silicate concentrations can be found around 3000 m, wedged between NEADW and NWABW, which indicates an influence of AABW in the form of Lower Deep Water (LDW\*). (b) Temperature-salinity diagrams with potential density  $\sigma_0$  contours for Orphan Knoll and Rockall Plateau. In the Feni Drift temperature-salinity diagram the open square and circle represent LDW (2.42°C, 34.9) and ISOW (1.8°C, 35.0) end-members as defined by Van Aken and De Boer [1995].

AMS  $^{14}\text{C}$  dates for the two locations can be found in the auxiliary material. Conversion to calendar years before present (cal. yr BP) was with CALIB 501 [Stuiver and Reimer, 1993] using marine04 as calibration data set. Mean ages are the arithmetic means of the age ranges given by the program. The core locations experienced moderate to very high Holocene sedimentation rates, with average rates of 18 cm/ka (MD2024) and 150 cm/ka (MD2251), respectively.

### 3. Regional Hydrography

[8] Both sites analyzed lie under the flow of the Deep Northern Boundary Current (DNBC) of McCartney [1992]. The DNBC comprises a set of deep western boundary currents between Scotland and Canada that originate from the Nordic Sea overflows. The combined overflows of Iceland-Scotland Overflow Water (ISOW), Denmark Strait Overflow Water (DSOW), and LSW, flow south out of Labrador Sea as proto-NADW in the North Atlantic's Western Boundary

Undercurrent (WBUC). The Orphan Knoll site (MD2024) is presently under the influence of Northwest Atlantic Bottom Water (NWABW), which is the coldest and densest North Atlantic water mass (Figure 2), albeit of lower salinity than Northeast Atlantic Deep Water (NEADW). NWABW contains mainly DSOW, plus some LSW, Subpolar Mode Water (SPMW) and a trace of Mediterranean Water [Frew *et al.*, 2000] entrained on its descent from Denmark Strait, reaching water depths below 4 km in the North Atlantic. The NE Atlantic is under the influence of NEADW, which is the second densest North Atlantic water mass (Figure 2). NEADW typically occupies water depths of 2.0–3.5 km in the eastern basin and 1.7–3.0 km in the western basin, comprising ISOW originating from the eastern Greenland-Iceland-Norwegian (GIN) Seas [Hansen and Østerhus, 2000], with entrained LSW and SPMW [Frew *et al.*, 2000]. Intermediate waters (0.5 to 2.0 km) in the North Atlantic are made up of LSW with lower density than NEADW and NWABW, and are mainly formed by wintertime convection

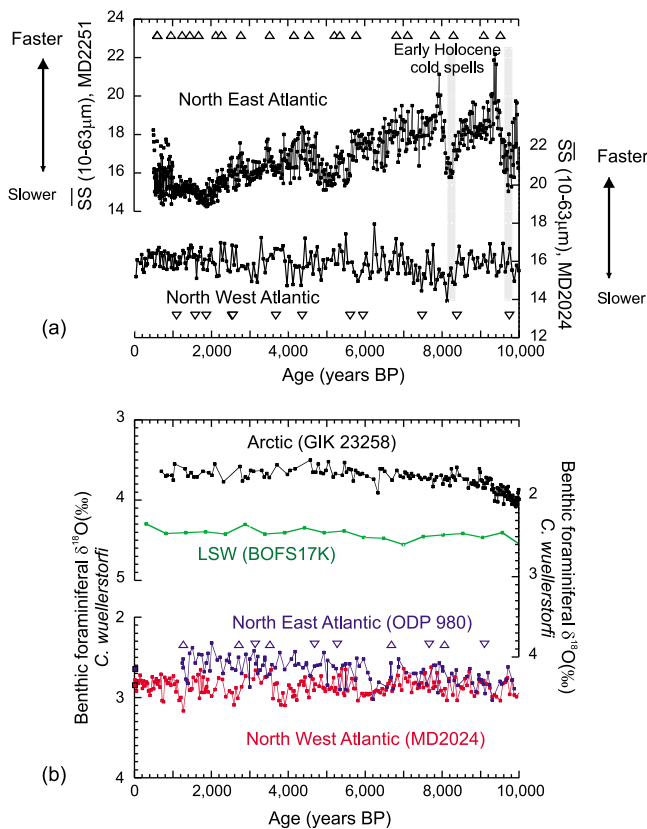


**Figure 3.** (a) Mean grain sizes for the sortable silt fraction (10–63  $\mu\text{m}$ ) for MD2251 and MD2024 with MD2251 showing a long-term decrease in mean grain sizes after 6,500 years. The enhanced variability near the core top of MD2251 (top 1.7 m, last 1,000 years) is most probably an artifact. Also shown are calibrated radiocarbon ages ( $\Delta$  MD2251;  $\nabla$  MD2024). (b) Benthic foraminiferal  $\delta^{18}\text{O}_c$  records from locations presently bathed in Norwegian Sea Deep Water (23258–3 from *Sarnthein et al.* [2003]), LSW (BOFS17K from *Bertram et al.* [1995]), NEADW (ODP 980 from *Oppo et al.* [2003]), and NWABW (MD2024). Location details can be found in Table 1. Calibrated radiocarbon ages ( $\nabla$  *G. bulloides*  $\Delta$  *N. pachyderma* (r)) are shown for ODP 980. Red and blue squares at 0 years show predicted present-day benthic foraminiferal  $\delta^{18}\text{O}_c$  (from seawater temperature and  $\delta^{18}\text{O}_{\text{sw}}$  using *Bemis et al.*'s [1998] equation) for MD2024 and ODP 980 respectively. Present-day bottom water temperature at MD2024 is 2°C (Figure 2);  $\delta^{18}\text{O}_{\text{sw}}$  of NWABW is 0.15‰ [Frew et al., 2000]. At ODP 980 present-day bottom water temperature is 3.5°C (Figure 2) and  $\delta^{18}\text{O}_{\text{sw}}$  of NEADW is 0.22‰ [Frew et al., 2000].

in the Labrador Sea (Figure 2). Within the northern North Atlantic enhanced silicate concentrations around 3000 m in LDW, evident in Labrador Sea as well as the Eastern Atlantic are diagnostic for an influence of AABW [McCartney, 1992].

#### 4. Results

[9] The flow speed reconstructions at sites MD2024 and MD2251 show quite different behavior during the Holocene

(Figure 3a). Our reconstructions show fast NEADW flow speeds during the early Holocene, briefly interrupted during short cold spells of the early Holocene (cf. the 9.7 ka event identified by *Bond et al.* [2001] and the 8.2 ka event [Ellison et al., 2006], captured in Greenland ice records [e.g., Thomas et al., 2007]). After  $\sim 6,500$  years the flow speed of the DNBC along Gardar Drift (MD2251) that feeds NEADW shows a gradual decline until 1,000 years ago. Flow vigor reconstructions of core NEAP-15K [Bianchi and McCave, 1999], nearby from Southern Gardar Drift and under the influence of NEADW, also show a decline in average silt size over this time interval, but to a much smaller extent. Core MD2251 is from an area characterized by strong current action in vicinity of the fast flowing core of the current, whereas NEAP-15K is not [Bianchi and McCave, 2000]. The sortable silt record of MD2251 is therefore likely to be more sensitive to small changes in flow vigor that occurred during the Holocene. The gradual decline in NEADW flow speed is interrupted by short intervals of reduced flow speed around 6,300, 5,500, 5,200–4,800, 3,700, 3,000 and 1,900 years ago (Figure 3a).

[10] In contrast, flow speed variations at MD2024 (presently influenced by NWABW) are less dramatic, showing only a slight increase between 8,400 and 6,800 years ago (Figure 3a). At MD2024 the occurrence of coarse lithic grains (diameter  $> 250 \mu\text{m}$ ) provides evidence for associated ice rafting  $\sim 7,800$  years, but the accumulation rate shows no perturbation that might invalidate inferences from sortable silt measurements (auxiliary material). Between 8,000 and 5,800 years ago flow speed variations at the two sites may be anti-phased: between 8,000 and 6,000 years ago MD2024 shows an increasing trend whereas MD2251 shows a decreasing trend, followed by a decrease at MD2024 flow vigor  $\sim 5,800$  years ago and invigorated flow speed of MD2251 (Figure 3a).

[11] The benthic foraminiferal  $\delta^{18}\text{O}_c$  records of MD2024 (presently influenced by NWABW) and ODP 980 (on Feni Drift to the east of core MD2251 and influenced by NEADW) show similar values (means of  $2.85 \pm 0.10\text{‰}$  versus  $2.76 \pm 0.12\text{‰}$  respectively) during the early Holocene between 10,000 and 6,500 years (Figure 3b). After 7,000 years  $\delta^{18}\text{O}_c$  increases to 3.0‰ at both locations, followed by an abrupt decrease to 2.8‰ and 2.6‰ respectively around 6,500 years (Figure 3b; note that the absence of any radiocarbon dates between 6,670 and 5,240 years at ODP 980 precludes assessment of leads and lags between the two sites). For the remainder of the Holocene  $\delta^{18}\text{O}_c$  at MD2024 fluctuates around  $2.87 \pm 0.11\text{‰}$  with intervals of increased (to 3‰)  $\delta^{18}\text{O}_c$  centered around 3,800, 2,500 and 1,200 years and decreased  $\delta^{18}\text{O}_c$  centered around 3,200 years, whereas those of ODP 980 remain much more depleted around  $2.60 \pm 0.13\text{‰}$  (Figure 3b). Depleted ( $-0.2\text{‰}$ ) benthic foraminiferal  $\delta^{18}\text{O}_c$  after 6,500 years also can be observed in other, lower resolution benthic records with poorer age constraints from locations bathed in ISOW (south of Iceland) and NEADW (Feni Drift; see auxiliary material).

[12] Inclusion of an ice-volume correction between 10,000 and 7,000 years ago (melting of ice sheets over that period resulted in a 40 m sea level rise; see review of *Stanford et al.* [2011]) results in slightly more depleted  $\delta^{18}\text{O}_c$  values (2.5‰ NEADW, 2.6‰ NWABW) during the early Holocene (until

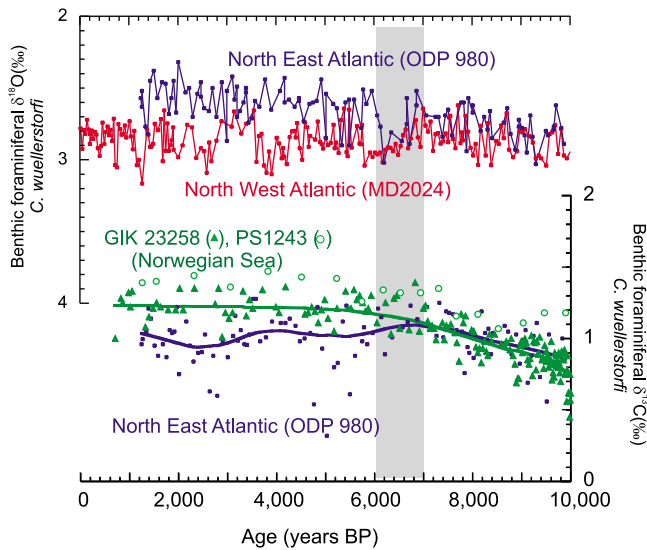


**Figure 4.** Benthic foraminiferal  $\delta^{18}\text{O}_c$  of MD2024 (presently NWABW) and ODP 980 (NEADW), and benthic foraminiferal  $\delta^{13}\text{C}$  of ODP 980 (blue circles [Oppo *et al.*, 2003]) from Feni Drift, and cores 23258–3 (green triangles [Sarnthein *et al.*, 2003]) and PS1243 (open green circles [Bauch *et al.*, 2001]) from the Norwegian Sea. Thick blue and green lines (results of a least squares *Stineman* [1980] function with 33% smoothing applied to  $\delta^{13}\text{C}$  data of cores ODP 980 and 23258–3 respectively) illustrate the development of a  $\delta^{13}\text{C}$  gradient between the Norwegian Sea and NEADW after 7,000 years.

~7,000 years), increasing to 3‰ around 6,500 years. However, due to the core locations' proximity to the Laurentide and Eurasian Ice Sheets, a stronger meltwater effect than estimated from dilution to the whole ocean would be expected, and ice-volume corrections in this region will thus carry relatively large uncertainties.

[13] The benthic foraminiferal  $\delta^{13}\text{C}$  record of ODP 980 shows identical values and trends to those of cores from the Norwegian Sea (cores 23258–3 and PS1243) until 7,000 years, whereas after 7,000 those of ODP 980 become depleted by  $-0.2$  to  $-0.3$ ‰, creating a  $\delta^{13}\text{C}$  gradient between the two regions (Figure 4). A similar reduction in deep  $\delta^{13}\text{C}$  after

6,000 is also a feature of the Southern Rockall transect of Sarnthein *et al.* [2001].

## 5. Discussion

### 5.1. Long-Term Hydrographic and Flow Speed Changes

[14] Benthic foraminiferal  $\delta^{18}\text{O}_c$  at MD2024 and ODP 980 show similar trends and values until ~6,500 years ago, but diverge thereafter (Figure 3b). We consider these changes in benthic  $\delta^{18}\text{O}_c$  to be related to changes in bottom water properties (mainly seawater oxygen isotopes ( $\delta^{18}\text{O}_{\text{sw}}$ ) and temperature), rather than secondary effects related to preservation (dissolution) effects, kinetic fractionation effects or vital effects. Only well preserved specimens of *C. wuellerstorfi* were selected for isotope analysis at MD2024, and cores bathed in NEADW are all located well above the lysocline (Table 1). Through the use of, and comparison with, monospecific samples of *C. wuellerstorfi*, uncertainties relating to vital effects should be avoided. Furthermore variations in carbonate ion concentrations over the last 10,000 years were probably minimal [Yu *et al.*, 2008], excluding kinetic fractionation effects as a cause.

[15] The mid-to-late Holocene depleted benthic foraminiferal  $\delta^{18}\text{O}_c$  at locations bathed in NEADW are not related to changes in the physical properties of ISOW, as depleted benthic foraminiferal  $\delta^{18}\text{O}_c$  is not observed at sites bathed in Norwegian Sea Deep Water (NSDW) (Figure 3b), a source water for ISOW. It is also unlikely that changes in the properties of entrained water masses (i.e., LSW or SPMW) are responsible for the depleted values. For example, no change is observed in the BOFS 17K benthic foraminiferal  $\delta^{18}\text{O}_c$  record [Bertram *et al.*, 1995], which at 1150 m is under the influence of LSW. Subpolar mode waters may have been cooler and less dense during the early Holocene (9,000 to 6,000 years) by  $1^\circ\text{C}$  and  $0.4\text{ kg/m}^3$  [Thornalley *et al.*, 2009], but the two effects cancel each other out, with no difference between early and late Holocene planktonic foraminiferal  $\delta^{18}\text{O}_c$ .

[16] Presently NWABW is denser than NEADW because it is considerably cooler, albeit fresher (Figure 2b). Similar values and trends in  $\delta^{18}\text{O}_c$  of benthic foraminifera from ODP 980 and MD2024 between 10,000 and 6,500 years could indicate that their water mass properties were more similar, compared with the last 6,500 years. A weak eastward flow, originating from the northwest Atlantic, has been detected in

**Table 1.** Details of Core Locations Discussed in This Study

Core	Latitude	Longitude	Water Depth (km)	Region	Water Mass	Reference
GIK- 23258	75.0	14.0	1.78	Barents Sea Slope	Norwegian Sea Deep Water	Hirschleber <i>et al.</i> [1988], Sarnthein <i>et al.</i> [2003]
PS 1243–1/2	69°22.3	06°32.1	2.71	Central Norwegian Sea	Norwegian Sea Deep Water	Bauch <i>et al.</i> [2001]
BOFS 17K	58.0	−16.5	1.15	Hatton-Rockall basin	LSW	McCave [1989]
ODP 980	55.5	−14.7	2.17	Rockall Plateau	NEADW	Shipboard Scientific Party, [1996], Oppo <i>et al.</i> [2003]
RAPiD-12-1K	62.1	−17.8	1.94	East Katla Ridge	NEADW	McCave [2005], Thornalley <i>et al.</i> [2010]
MD99-2251	57.5	−27.9	2.62	Gardar Drift flank	NEADW	Hillaire-Marcel and Turon [1999], this study, Ellison <i>et al.</i> [2006]
MD03-2665	57.5	−48.6	3.44	Eirik Drift	NWABW	Kleiven <i>et al.</i> [2008]
MD95-2024	50.2	−45.7	3.49	Orphan Knoll	NWABW	Bassinot and Labeyrie [1996], this study

the Charlie-Gibbs Fracture Zone (CGFZ) recently, where NWABW occupies the bottom of the southern trough of CGFZ [Saunders, 1994]. Features of the flow are strongly episodic pulses of warm/salty flow to the west and weaker pulses of cool/fresh water flow to the east. However, the hydrography of the eastern basins is presently not significantly influenced by this process [McCartney, 1992]. In the face of a strong Coriolis-forced boundary current coming from Gardar Drift during the early Holocene as indicated by the mean grain sizes (Figure 3a), it is unlikely that a sufficiently powerful reverse flow caused NWABW to occupy both MD2024 and ODP 980 locations as it would have required this water to fill up the eastern basin to ~2000 m.

[17] *Van Aken and De Boer* [1995] and *Frew et al.* [2000] show, based on hydrographic and isotope data, that NEADW is mainly composed of ISOW with entrained SPMW, LSW and LDW. In the Rockall Trough above a bottom LDW layer with 30  $\mu\text{mol/kg}$  silica, NEADW has somewhat higher Si (15  $\mu\text{mol/kg}$ ) than the 10  $\mu\text{mol/kg}$  found in Norwegian Sea Deep Water [Lonsdale and Hollister, 1979], suggesting that NEADW at ODP 980 may thus contain up to 25% of LDW. Seawater  $\delta^{18}\text{O}_{\text{sw}}$  of ISOW (0.3‰ [Östlund and Hut, 1984]) and SPMW (0.3‰ [Frew et al., 2000]) are identical, and so with a NEADW  $\delta^{18}\text{O}_{\text{sw}}$  of 0.22‰, LDW of 0.13‰ and LSW of 0.10‰ [Frew et al., 2000] we calculate that NEADW at Feni Drift (location of ODP 980) contains ~20% of entrained LSW and 55% of ISOW/SPMW. Average temperatures of SPMW, ISOW, LDW and LSW are 8°C, 1.8°C, 2.4°C, 3.4°C respectively [Van Aken and De Boer, 1995]. Given the NEADW temperature of 3.5°C at the site of ODP 980, we estimate that NEADW here contains ~35% ISOW and 20% entrained SPMW.

[18] Reductions in entrained LSW or LDW within NEADW relative to modern values, and an increase in the proportion of ISOW, would result in an increase in NEADW  $\delta^{18}\text{O}_{\text{sw}}$  and salinity and a reduction in temperature. Complete removal of LSW and LDW from NEADW at ODP 980, compensated for by an increased proportion of ISOW (raised to 80%), would increase NEADW  $\delta^{18}\text{O}_{\text{sw}}$  and salinity by 0.08‰ and 0.05 respectively, and cause a 0.5°C decrease in temperature, giving a  $\delta^{18}\text{O}_{\text{c}}$  increase of 0.2‰. Following *Frew et al.*'s [2000] present-day NEADW and NWABW end-members (salinities of 34.96 and 34.88, and temperatures of 2.8°C and 1.25°C, giving potential densities  $\sigma_0$  of 23.87 and 27.93); a 0.5°C decrease in NEADW temperature and a 0.05 increase in salinity would raise NEADW  $\sigma_0$  to 27.96, making NEADW density similar to or slightly higher than that of NWABW during the early Holocene. This would imply that there was no density gradient between NWABW and NEADW during the early Holocene, or that it was reversed. In the latter case NEADW would underlie NWABW, and potentially occupy water depths currently occupied by NWABW (including the location MD2024) in the northwest Atlantic. Our results are supported by a geochemical sediment provenance study by *Fagel et al.* [2004], who suggested that NWABW became the dominant bottom water mass in the Labrador Sea only after 6,500 years. This does not necessarily exclude the existence of NWABW in the northwest Atlantic during the early Holocene; it may just have occupied shallow water depths compared with today.

[19] From the above discussion it seems possible that absence of entrained LDW and LSW waters from NEADW in

the northeast Atlantic Basin may have been the cause for heavier benthic foraminiferal  $\delta^{18}\text{O}_{\text{c}}$  during the early Holocene. Is there any further evidence to substantiate this? Carbonate ion reconstructions of *Yu et al.* [2008] at the deeper sites in the northeast Atlantic Basin show highest carbonate ion concentrations during the early Holocene, followed by somewhat decreased values, pointing to a slightly lower carbonate ion water mass during the mid- to late Holocene. Furthermore, while the benthic foraminiferal  $\delta^{13}\text{C}$  values at ODP 980 are almost identical to those from Nordic Seas core 23258–3 during the early Holocene, after 7,000 years the benthic  $\delta^{13}\text{C}$  at ODP 980 decreases by 0.2‰, in concert with the  $\delta^{18}\text{O}_{\text{c}}$  increase at both sites (Figure 4). As carbonate ion concentrations of LDW are much lower compared with those of NADW, and LDW is the highest nutrient/lowest  $\delta^{13}\text{C}$  deep water mass in the North Atlantic basin, we propose that the  $\delta^{13}\text{C}$  gradient that developed between Norwegian Sea core 23258–3/PS 1243 and ODP 980 is the result of shoaling of LDW in the northeast Atlantic Basin after 7,000 years.

[20] Although LSW/NEADW stratification became established early during the Holocene, active modern-like LSW production started ~7,000 years ago [Hillaire-Marcel et al., 2001]. Potentially increased LSW production after ~7,000 years resulted in deeper eastward transport of LSW and entrainment into NEADW along the overflows.

[21] We observe a long-term decrease in the mean silt grain size at MD2251 from around 6,500 years coincident with the hydrographic changes in the deep northeast Atlantic Basin (Figure 3). The amplitude of fluctuations in the flow speed also decreases markedly from that time, with variations of up to 3.5 standard deviation before 7,000 years but little more than 1 SD thereafter (Figure 5a). The long-term decrease in silt grain size at MD2251, located near the fast flowing core of the current, points to a reduction in the flow speed of the DNBC or a migration of its major flow axis since ~6,500 years.

[22] Lighter benthic foraminiferal  $\delta^{18}\text{O}_{\text{c}}$  at sites bathed in NEADW and the development of a  $\delta^{13}\text{C}$  gradient between the Norwegian Sea and S. Iceland Basin after ~7,000 years suggests a possible increased influence of LDW and LSW in NEADW (Figures 3 and 4). The decrease in flow vigor observed at MD2251 may thus be caused by weakened flow of the eastern component of the DNBC rather than a migration of its major flow axis. At Katla Ridge (South of Iceland), *Thornalley et al.* [2010] observe an increase in weight % sand after ca 7,500 years, which they attribute to an increase in ISOW current strength, which could be related to a shoaling of the ISOW current.

[23] In the deep northwest Atlantic Basin, grain sizes at MD2024 increase slightly after 8,000 years, but overall no large scale flow speed changes are observed over the Holocene (Figure 3a). This suggests that, on the long-term, flow speed at MD2251 and MD2024 are not coordinated. This may be because MD2251 is more a recorder of overflow changes (being closer to the source), whereas MD2024 may represent a more mature assembled flow much further downstream from the overflows. It is also surprising that there was no significant change in flow speed at MD2024 after 6,500 years when the site may have switched from being influenced by NEADW to being influenced by predominantly NWABW. On the other hand, NEADW flow speed and properties may be linked to LSW production; active

production of LSW  $\sim 7,000$  years coincides with the long-term reduction in NEADW flow speed.

[24] The changes observed in NEADW may be related to high latitude insolation changes. During the early Holocene, high summer insolation and a strong inflow of North Atlantic surface waters caused a reduction in Arctic Sea ice, and may

have contributed to increased deep water formation in the Nordic Seas [Rasmussen *et al.*, 2002; Renssen *et al.*, 2005; Polyak *et al.*, 2010; Ślubowska-Woldengen *et al.*, 2007]. It is likely that this would have resulted in stronger NEADW flow. After ca. 7,000 years, a reduction in high latitude summer insolation was responsible for a general North Atlantic cooling trend [Moros *et al.*, 2004] and an increase in Arctic Sea ice [Polyak *et al.*, 2010], causing strong freshening in the Nordic Seas and a reduction in deep water formation [Renssen *et al.*, 2005] and NEADW flow strength. However, Renssen *et al.* [2005] argue that the enhanced meridional temperature gradient that resulted from the decrease in high latitude insolation, caused a strengthening of the Westerlies, which promoted further cooling in the Labrador Sea area causing increased deep water formation there. Over shorter time scales (years to decades) NEADW flow and LSW production may also be linked, with higher LSW production provoking slower overflow current speeds [Boessenkool *et al.*, 2007].

[25] The model simulation by Renssen *et al.* [2005] does not show an overall change in AMOC during the Holocene. Holocene flow speed and hydrographic reconstructions of proto-NADW in the WBUC south of the Labrador Sea are critical to assess the effects that the observed changes in NEADW and NWABW properties and flow have on the overall AMOC.

## 5.2. Short-Term Flow and Hydrographic Changes

[26] Shorter-term flow speed variability is pronounced at site MD2251 bathed in NEADW with several abrupt large-scale slow-downs at 10,400–10,100, 9,850–9,600, 8,450–8,050, 5,200–4,800, 3,300–2,950 and 2,100–1,700 years, and some of smaller-scale at 6,600–~6,250, 5,630–5,450, and 3,850–3,630 (Figures 3 and 5a). At MD2024 smaller-scale shorter-term flow speed slow downs may be observed around 9,800, 8,400–7,800, 7,600–7,000, 6,000–5,600, 4,800, 4,500–3,900, 2,200, and 500 years to present. The timing of several of the slow-downs can potentially be linked to Bond *et al.*'s [2001] drift ice events, for which a number of forcing mechanism have been proposed (e.g., Debret *et al.* [2007] oceanic forcing versus Bond *et al.* [2001] solar forcing).

[27] Wavelet spectral analysis was used to analyze variability of non-stationary processes of the sortable silt records, using the procedures of Maraun *et al.* [2007]. It has the important advantage over Fourier transforms that it identifies both frequency and location in time. The wavelet

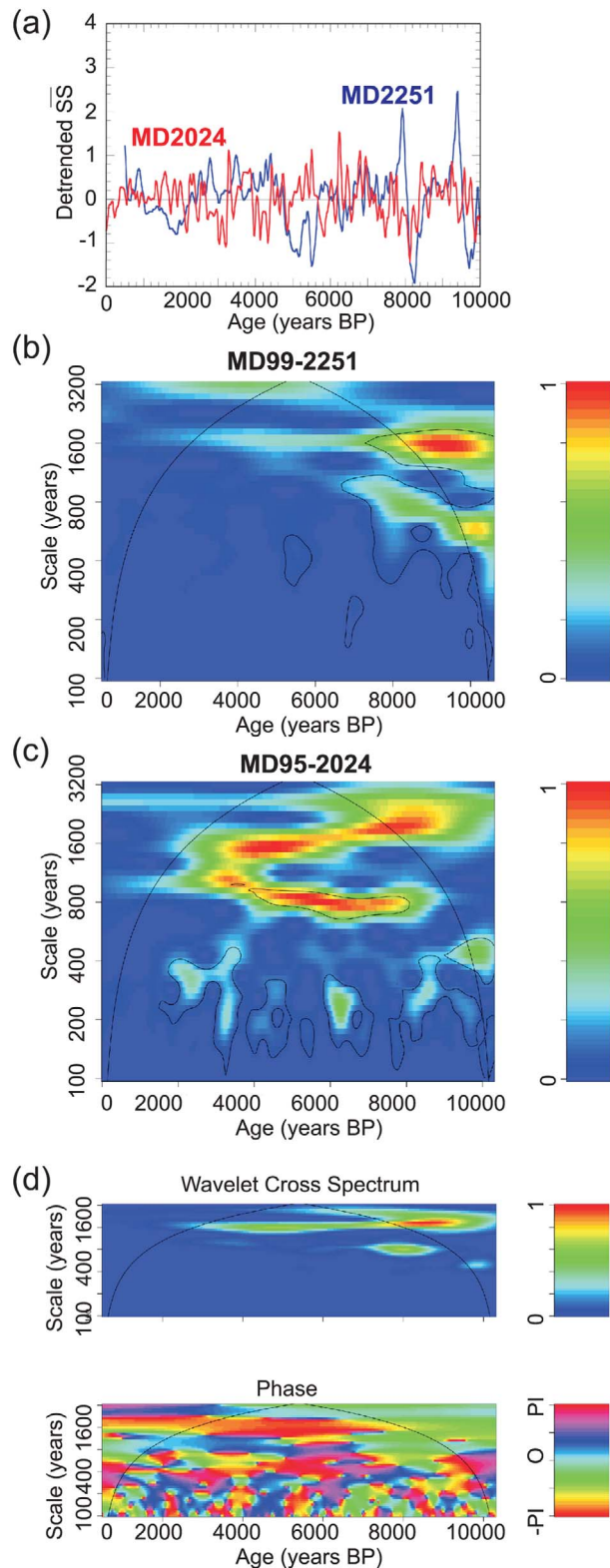


**Figure 5.** (a) De-trended mean grain sizes for MD2251 and MD2024 suggest similar millennial trends in flow vigor at both locations during the early Holocene (until 6,500 years ago), followed by mainly opposing trends after. Raw mean grain size data of sortable silt fraction ( $10\text{--}63\ \mu\text{m}$ ) were smoothed with a 150 year Gaussian window and then de-trended using a fourth order polynomial. (b, c) Wavelet analysis of MD2251 and MD2024 de-trended sortable silt data. Analyses were conducted using the R package SOWAS [Maraun *et al.*, 2007], areas enclosed by the solid line indicate pointwise significance at the 95% level. (d) Cross spectral wavelet wavelet coherence (top) and phase relationship (bottom) of MD2251 and MD2024.

spectrum of the MD2251 record shows a 1600 year periodicity during the early Holocene, whereas that of MD2024 shows 800 and 1600 year periodicities between 8,000 and 3,000 years (Figure 5). Core MD2251 is not far from NEAP 15K in which *Bianchi and McCave* [1999] recorded a 1500 year periodicity in grain size, whereas *Chapman and Shackleton* [2000] observed periods of 1600, 1000 and 550 years in sediment lightness. These periodicities were confirmed by *Debret et al.* [2007] using wavelet analysis. Although the wavelet analysis of MD2251 shows a consistent 1600-year band across the spectrum it is mainly below the 95% confidence limit (Figure 5b). The wavelet analysis of MD2024 identifies 800 and 1600 year periods in the early to late Holocene with the 800 year signal exceeding the 95% confidence levels between 8,000 and 3,000 years (Figure 5b). However, it is noted that most of the changes in mean grain size at the site fall close to the analytical precision of 1.5%. Interestingly, the wavelet cross spectrum suggest that the records are coherent in the 1600 year band during the early Holocene (Figure 5d).

[28] Taking into account dating uncertainties (reservoir ages, interpolation technique) the two flow speed reconstructions may show similar trends during the early Holocene (until ~6,500 years ago), followed by predominantly opposing trends thereafter (Figure 5a, however note that anti-phase relationship may not be supported by wavelet analysis). This observation may indicate a potential influence of NEADW rather than NWABW at the Orphan Knoll Site until 6,500 years. Why the two sites might show opposing trends after 6,500 years (excluding interval 3,600 and 2,200 years) is puzzling. The strength of subpolar gyre circulation may depend on local wind stress and/or buoyancy forcing [*Häkkinen and Rhines*, 2004]. In a modeling study *Biajstoch et al.* [2003] suggested that a higher wind-forcing would lead to an increased flux of DSOW and a decrease in ISOW, so increased flow speed of NWABW (fed by DSOW) and decreased flow speed of NEADW (fed by ISOW) could result from higher wind-forcing, with the opposite pattern related to decreased wind strength. Blackman-Tukey cross-spectral analysis shows no statistically significant shared periodicities between the two records, so neither confirm nor deny the suspicion of anti-phase relationships from visual inspection of the records.

[29] Most of the shorter-term changes in flow speed do not coincide with changes in benthic  $\delta^{18}\text{O}_c$ , apart from the interval 3,500 to 2,800 at MD2024 where depleted  $\delta^{18}\text{O}_c$  appears to be accompanied by slower flow (Figure 3). This interval of depleted  $\delta^{18}\text{O}_c$  at MD2024 is not an outlier as its timing is identical to that of an interval of depleted  $\delta^{18}\text{O}_c$  at Eirik Drift in core MD03–2665 of *Kleiven et al.* [2008] in the Labrador Sea. As there was no associated decrease in benthic  $\delta^{13}\text{C}$ , it is unlikely that this  $\delta^{18}\text{O}_c$  depletion was related to a shoaling of LDW in the northwest Atlantic. Instead it may result from the increased entrainment of a less dense (warmer or fresher) water in NWABW, most likely LSW.

## 6. Conclusions

[30] High resolution flow speed reconstructions of two core sites located on Gardar Drift in the northeast Atlantic and Orphan Knoll in the northwest Atlantic show contrasting long-term and short-term trends during the Holocene. While

core MD2251 reveals a long-term decrease in flow speed of NEADW from ~6,500 years, long-term flow vigor at MD2024 shows no substantial long-term changes. Benthic  $\delta^{18}\text{O}_c$  of sites from the northeast (ODP 980) and northwest Atlantic (MD95–2024) show similar trends and values during the early Holocene (until 6,500 years) but diverge afterwards, with  $\delta^{18}\text{O}_c$  values from the northeast Atlantic being ~0.27‰ more depleted than those from the northwest Atlantic Basin. A  $\delta^{13}\text{C}$  gradient between NSDW (source for ISOW which feeds NEADW) and NEADW itself also begins to develop ~7,000 years ago. We relate these changes in benthic foraminiferal isotopes bathed in NEADW to a shoaling of LDW whose ultimate source is AABW, in combination with a deeper eastward advection of LSW in the northeast Atlantic Basin. We propose that the absence of a  $\delta^{13}\text{C}$  gradient during the early Holocene indicates that LDW was of only minor importance in the North Atlantic Basin, and that a weakened NEADW flow (as indicated by our flow vigor record) during the mid to late Holocene, allowed the penetration of LDW into the northeast Atlantic Basin.

[31] **Acknowledgments.** We are especially grateful to Gillian Foreman, Jo Hellewell, Angela Huckle and Johannes Simstich for assistance with sample processing. Mike Hall provided valuable advice on isotope measurements. Thanks to Stuart Painter from the National Oceanography Centre in Southampton for help with calculating density lines. AMS radiocarbon dates for cores MD95 2024 and HU91 045 093 were provided by the NERC RAPID program (grant NER/T/S/2002/00436 to INMcC). BAAH was funded by PACLIVA (EU project grant EVK2-2002-00143 to INMcC) and the Newton Trust in Cambridge. The cores used in this study were collected as part of the IMAGES program. We are grateful for constructive reviews by three anonymous reviewers as well as the Editor (Rainer Zahn).

[32] All new data will be made available upon publication through <http://www.ncdc.noaa.gov>.

## References

- Bassinot, F., and L. Labeyrie (1996), *Campagne IMAGES MD 101*, 217 pp., Inst. Fr. Rech. Pour Technol. Polaires, Plouzané, France.
- Bauch, H. A., H. Erlenkeuser, R. F. Spielhagen, U. Struck, J. Matthiessen, J. Thiede, and J. Heinemeier (2001), A multiproxy reconstruction of the evolution of deep and surface waters in the subarctic Nordic seas over the last 30,000 yr, *Quat. Sci. Rev.*, 20, 659–678, doi:10.1016/S0277-3791(00)00098-6.
- Bemis, B. E., H. J. Spero, J. Bijma, and D. W. Lea (1998), Reevaluation of the oxygen isotopic composition of planktonic foraminifera: Experimental results and revised paleotemperature equations, *Paleoceanography*, 13, 150–160, doi:10.1029/98PA00070.
- Bertram, C. J., H. Elderfield, N. J. Shackleton, and J. A. MacDonald (1995), Cadmium/calcium and carbon isotope reconstructions of the glacial northeast Atlantic Ocean, *Paleoceanography*, 10, 563–578, doi:10.1029/94PA03058.
- Bianchi, G. G., and I. N. McCave (1999), Holocene periodicity in North Atlantic climate and deep-ocean flow south of Iceland, *Nature*, 397, 515–517, doi:10.1038/17362.
- Bianchi, G. G., and I. N. McCave (2000), Hydrography and sedimentation under the deep western boundary currents on Björn and Gardar Drifts, Iceland Basin, *Mar. Geol.*, 165, 137–169, doi:10.1016/S0025-3227(99)00139-5.
- Bianchi, G. G., I. R. Hall, I. N. McCave, and L. Joseph (1999), Measurement of the sortable silt current speed proxy using the Sedigraph 5100 and Coulter Multisizer II: Precision and accuracy, *Sedimentology*, 46, 1001–1014, doi:10.1046/j.1365-3091.1999.00256.x.
- Biajstoch, A., R. H. Käse, and D. B. Stammer (2003), The sensitivity of Greenland-Scotland Ridge overflow to forcing changes, *J. Phys. Oceanogr.*, 33, 2307–2319, doi:10.1175/1520-0485(2003)033<2307:TSOTGR>2.0.CO;2.
- Boessenkool, K. P., I. R. Hall, H. Elderfield, and I. Yashayaev (2007), North Atlantic climate and deep-ocean flow speed changes during the last 230 years, *Geophys. Res. Lett.*, 34, L13614, doi:10.1029/2007GL030285.

- Bond, G., B. Kromer, J. Beer, R. Muscheler, M. N. Evans, W. Showers, S. Hoffmann, R. Lotti-Bond, I. Hajdas, and G. Bonani (2001), Persistent solar influence on North Atlantic climate during the Holocene, *Science*, *294*, 2130–2136, doi:10.1126/science.1065680.
- Boyer, T. P., J. I. Antonov, H. E. Garcia, D. R. Johnson, R. A. Locarnini, A. V. Mishonov, M. T. Pitcher, O. K. Baranova, and I. V. Smolyar (2006), *World Ocean Database 2005* [DVDs], edited by S. Levitus, 190 pp., *NOAA Atlas NESDIS, vol. 60*, U.S. Gov. Print. Office, Washington, D. C.
- Broecker, W., and E. Clarke (2007), Is the magnitude of the carbonate ion decrease in the abyssal ocean over the last 8 kyr consistent with the 20 ppm rise in atmospheric CO<sub>2</sub> content?, *Paleoceanography*, *22*, PA1202, doi:10.1029/2006PA001311.
- Chapman, M. R., and N. J. Shackleton (2000), Evidence of 550-year and 1000-year cyclicity in North Atlantic circulation patterns during the Holocene, *Holocene*, *10*, 287–291, doi:10.1191/095968300671253196.
- Debrat, M., V. Bout-Roumazeilles, F. Grousset, M. Desmet, J. F. McManus, N. Massei, D. Sebag, J.-R. Petit, Y. Copard, and A. Trentesaux (2007), The origin of the 1500-year climate cycles in Holocene North Atlantic records, *Clim. Past*, *3*, 569–575, doi:10.5194/cp-3-569-2007.
- Ellison, C. R. W., M. R. Chapman, and I. R. Hall (2006), Surface and deep ocean interactions during the cold climate event 8200 years ago, *Science*, *312*, 1929–1932, doi:10.1126/science.1127213.
- Fagel, N., C. Hillaire-Marcel, M. Humblet, R. Brasseur, D. Weis, and R. Stevenson (2004), Nd and Pb isotope signatures of the clay size fraction of Labrador Sea sediments during the Holocene: Implications for the inception of the modern deep circulation pattern, *Paleoceanography*, *19*, PA3002, doi:10.1029/2003PA000993.
- Frew, R. D., P. F. Dennis, K. J. Heywood, M. P. Meredith, and S. M. Boswell (2000), The oxygen isotope composition of water masses in the northern North Atlantic, *Deep Sea Res., Part I*, *47*, 2265–2286, doi:10.1016/S0967-0637(00)00023-6.
- Gutjahr, M., M. Frank, C. H. Stirling, L. D. Keigwin, and A. N. Halliday (2008), Tracing the Nd isotope evolution of North Atlantic Deep and Intermediate Waters in the western North Atlantic since the Last Glacial Maximum from Blake Ridge sediments, *Earth Planet. Sci. Lett.*, *266*, 61–77, doi:10.1016/j.epsl.2007.10.037.
- Häkkinen, S., and P. B. Rhines (2004), Decline of subpolar North Atlantic circulation during the 1990s, *Science*, *304*, 555–559, doi:10.1126/science.1094917.
- Hall, I. R., G. G. Bianchi, and J. R. Evans (2004), Centennial to millennial scale Holocene climate-deep water linkage in the North Atlantic, *Quat. Sci. Rev.*, *23*, 1529–1536, doi:10.1016/j.quascirev.2004.04.004.
- Hansen, B., and S. Østerhus (2000), North Atlantic–Nordic seas exchanges, *Prog. Oceanogr.*, *45*, 109–208, doi:10.1016/S0079-6611(99)00052-X.
- Heegaard, E., H. J. B. Birks, and R. J. Telford (2005), Relationships between calibrated ages and depth in stratigraphical sequences: An estimation procedure by mixed-effect regression, *Holocene*, *15*, 612–618, doi:10.1191/0959683605hl836r.
- Hillaire-Marcel, C., and J.-L. Turon (1999), IMAGES V on board the *Marion Dufresne*, 2nd leg 30 June–24 July 1999, Rep. 99-X, 247 pp., Inst. Fr. Rech. Pour Technol. Polaires, Plouzané, France.
- Hillaire-Marcel, C., A. de Vernal, M. Lucotte, A. Mucci, G. Bilodeau, A. Rochon, S. Vallières, and G. Wu (1994), Productivité et flux de carbone dans la mer du Labrador au cours des derniers 40,000 ans, *Can. J. Earth Sci.*, *31*, 139–158, doi:10.1139/e94-012.
- Hillaire-Marcel, C., A. de Vernal, G. Bilodeau, and A. J. Weaver (2001), Absence of deep-water formation in the Labrador Sea during the last interglacial period, *Nature*, *410*, 1073–1077, doi:10.1038/35074059.
- Hirschleber, H., F. Theilen, W. Balzer, and B. von Bodungen (1988), *Forschungsschiff Meteor, Reise 7: Berichte der Fahrleiter*, Ber. SFB 313, vol. 10, 257 pp., Univ. Kiel, Kiel, Germany.
- Kleiven, H. F., C. Kissel, C. Laj, U. S. Ninnemann, T. O. Richter, and E. Cortijo (2008), Reduced North Atlantic Deep Water coeval with the glacial Lake Agassiz freshwater outburst, *Science*, *319*, 60–64, doi:10.1126/science.1148924.
- Laybeyrie, L., C. Waelbroeck, E. Cortijo, E. Michel, and J.-C. Duplessy (2005), Changes in deep water hydrology during the last deglaciation, *C. R. Geosci.*, *337*, 919–927, doi:10.1016/j.crte.2005.05.010.
- Lonsdale, P., and C. D. Hollister (1979), A near-bottom traverse of Rockall Trough: Hydrographic and geologic inferences, *Oceanol. Acta*, *2*, 91–105.
- Maraun, D., J. Kurths, and M. Holschneider (2007), Nonstationary Gaussian processes in wavelet domain: Synthesis, estimation and significance testing, *Phys. Rev. E*, *75*, 016707, doi:10.1103/PhysRevE.75.016707.
- McCartney, M. S. (1992), Recirculating components to the deep boundary current of the northern North Atlantic, *Prog. Oceanogr.*, *29*, 283–383, doi:10.1016/0079-6611(92)90006-L.
- McCave, I. N. (1989), *Cruise Report, RRS Discovery Cruise 184, 14 July–14 August 1989: BOFS 1989 Leg 3: Benthic Studies of the Biogeochemical Ocean Flux Study between 47°N and 60°N along 20°W in the Northeast Atlantic Ocean*, 38 pp., Dep. of Earth Sci., Univ. of Cambridge, Cambridge, U. K.
- McCave, I. N. (2005), *Cruise Report, RRS Charles Darwin Cruise 159, Rapid Climate Change*, 47 pp., Dep. of Earth Sci., Univ. of Cambridge, Cambridge, U. K.
- McCave, I. N., and I. R. Hall (2006), Size sorting in marine muds: Processes, pitfalls, and prospects for paleoflow-speed proxies, *Geochem. Geophys. Geosyst.*, *7*, Q10N05, doi:10.1029/2006GC001284.
- McCave, I. N., B. Manighetti, and S. G. Robinson (1995), Sortable silt and fine sediment size/composition slicing: Parameters for palaeocurrent speed and palaeoceanography, *Paleoceanography*, *10*, 593–610, doi:10.1029/94PA03039.
- Moros, M., K. Emeis, B. Risobrobakken, I. Snowball, A. Kuijpers, J. McManus, and E. Jansen (2004), Sea surface temperatures and ice rafting in the Holocene North Atlantic: Climate influences on northern Europe and Greenland, *Quat. Sci. Rev.*, *23*, 2113–2126, doi:10.1016/j.quascirev.2004.08.003.
- Oppo, D. W., J. F. McManus, and J. L. Cullen (2003), Paleo-oceanography: Deepwater variability in the Holocene epoch, *Nature*, *422*, 277–278, doi:10.1038/422277b.
- Östlund, H. G., and G. Hut (1984), Arctic Ocean water mass balance from isotope data, *J. Geophys. Res.*, *89*, 6373–6381, doi:10.1029/JC089iC04p06373.
- Polyak, L., et al. (2010), History of sea ice in the Arctic, *Quat. Sci. Rev.*, *29*, 1757–1778, doi:10.1016/j.quascirev.2010.02.010.
- Radi, T., and A. de Vernal (2008), Dinocysts as proxy of primary productivity in mid-high latitudes of the Northern Hemisphere, *Mar. Micropaleontol.*, *68*, 84–114, doi:10.1016/j.marmicro.2008.01.012.
- Rasmussen, T. L., D. Bäckström, J. Heinemeier, D. Klitgaard-Kristensen, P. C. Knutz, A. Kuijpers, S. Lassen, E. Thomsen, S. R. Troelstra, and T. C. E. van Weering (2002), The Faroe-Shetland gateway: Late Quaternary water mass exchange between the Nordic seas and the northeastern Atlantic, *Mar. Geol.*, *188*, 165–192, doi:10.1016/S0025-3227(02)00280-3.
- Renssen, H., H. Goosse, and T. Fichefet (2005), Contrasting trends in North Atlantic deep-water formation in the Labrador Sea and Nordic seas during the Holocene, *Geophys. Res. Lett.*, *32*, L08711, doi:10.1029/2005GL022462.
- Sarnthein, M., et al. (2001), Fundamental modes and abrupt changes in North Atlantic circulation over the last 60 ky—Concepts, reconstruction, and numerical modeling, in *The Northern North Atlantic*, edited by P. Schäfer et al., pp. 365–410, Springer, New York.
- Sarnthein, M., S. van Kreveld, H. Erlenkeuser, P. M. Grootes, M. Kucera, U. Pflaumann, and M. Schultz (2003), Centennial-to-millennial-scale periodicities of Holocene climate and sediment injections off the western Barents shelf, 75°N, *Boreas*, *32*, 447–461, doi:10.1111/j.1502-3885.2003.tb01227.x.
- Saunders, P. M. (1994), The flux of overflow water through the Charlie-Gibbs Fracture Zone, *J. Geophys. Res.*, *99*, 12,343–12,355, doi:10.1029/94JC00527.
- Schmidt, G. A., G. R. Bigg, and E. J. Rohling (1999), Global seawater oxygen-18 database: v1.20, <http://data.giss.nasa.gov/o18data/>, NASA Goddard Inst. for Space Stud., New York.
- Shipboard Scientific Party (1996), Sites 980/981, *Proc. Ocean Drill. Program Init. Rep.*, *162*, 49–90, doi:10.2973/odp.proc.ir.162.103.1996.
- Ślubowska-Woldengen, M., T. L. Rasmussen, N. Koç, D. Klitgaard-Kristensen, F. Nilsen, and A. Solheim (2007), Advection of Atlantic Water to western and northern Svalbard shelf since 17,500 cal yr BP, *Quat. Sci. Rev.*, *26*, 463–478, doi:10.1016/j.quascirev.2006.09.009.
- Stanford, J. D., R. Heminway, E. J. Rohling, P. G. Challenor, M. Medina-Elizalde, and A. J. Lester (2011), Sea-level probability for the last deglaciation: A statistical analysis of far-field records, *Global Planet. Change*, doi:10.1016/j.gloplacha.2010.11.002, in press.
- Stineman, R. W. (1980), A consistently well behaved method of interpolation, *Creat. Comput.*, *6*, 54–57.
- Stuiver, M., and P. J. Reimer (1993), Extended <sup>14</sup>C data base and revised CALIB 3.0 <sup>14</sup>C age calibration program, *Radiocarbon*, *35*, 215–230.
- Thomas, E. R., E. W. Wolff, R. Mulvaney, J. P. Steffensen, S. J. Johnsen, C. Arrowsmith, J. W. C. White, B. Vaughn, and T. Popp (2007), The 8.2 ka event from Greenland ice cores, *Quat. Sci. Rev.*, *26*, 70–81, doi:10.1016/j.quascirev.2006.07.017.
- Thornalley, D. J. R., H. Elderfield, and I. N. McCave (2009), Holocene oscillations in temperature and salinity of the surface subpolar North Atlantic, *Nature*, *457*, 711–714, doi:10.1038/nature07717.
- Thornalley, D. J. R., H. Elderfield, and I. N. McCave (2010), Intermediate and deep water paleoceanography of the northern North Atlantic over the

- past 21,000 years, *Paleoceanography*, 25, PA1211, doi:10.1029/2009PA001833.
- Van Aken, H. M., and C. J. De Boer (1995), On the synoptic hydrography of intermediate and deep water masses in the Iceland Basin, *Deep Sea Res., Part I*, 42, 165–189, doi:10.1016/0967-0637(94)00042-Q.
- Yu, J., H. Elderfield, and A. M. Piotrowski (2008), Seawater carbonate- $\delta^{13}\text{C}$  systematics and application to glacial-interglacial North Atlantic ocean circulation, *Earth Planet. Sci. Lett.*, 271, 209–220, doi:10.1016/j.epsl.2008.04.010.
- 
- B. A. A. Hoogakker, School of Geographic Sciences, University of Bristol, Bristol BS8 1SS, UK. (babette.hoogakker@gmail.com)
- M. R. Chapman and C. R. W. Ellison, School of Environmental Sciences, University of East Anglia, Norwich NR4 7TJ, UK.
- I. R. Hall, School of Earth and Ocean Sciences, University of Cardiff, Cardiff CF10 3AT, UK.
- C. Hillaire-Marcel, Centre GEOTOP, Université du Québec à Montréal, Montreal, Que. H3C 3P8, Canada.
- I. N. McCave, Department of Earth Sciences, University of Cambridge, Cambridge CB2 3EQ, UK.
- R. J. Telford, Department of Biology, University of Bergen, N-5020 Bergen, Norway.